

---

# An Information Theory of Compute-Optimal Size Scaling, Emergence, and Plateaus in Language Models

---

Anuj K. Nayak    Lav R. Varshney  
University of Illinois at Urbana-Champaign  
{anujk4, varshney}@illinois.edu

## Abstract

1        Recent empirical studies show three phenomena with increasing size of language  
2        models: *compute-optimal size scaling*, *emergent capabilities*, and *performance*  
3        *plateauing*. We present a simple unified mathematical framework to explain all of  
4        these language model scaling phenomena, building on recent skill-text bipartite  
5        graph frameworks for semantic learning. Modeling the learning of concepts from  
6        texts as an iterative process yields an analogy to iterative decoding of low-density  
7        parity check (LDPC) codes in information theory. Thence, drawing on finite-size  
8        scaling characterizations of LDPC decoding, we derive the compute-optimal size  
9        scaling (Chinchilla rule) for language models. Further, using tools from random  
10       network theory, we provide a simple explanation for both emergence of complex  
11       skills and plateauing of performance as the size of language models scale. We see  
12       multiple plateaus.

## 13    1 Introduction

14    To optimally use computational resources when training language models, several recent studies  
15    have empirically investigated how model size and dataset size should scale with compute budget  
16    [12, 9], finding a certain *allometric rule* much like in mathematical biology [24, 8]. As the sizes of  
17    language models continue to increase, large improvements in performance have been observed in  
18    certain complex tasks with only a small improvement in the model’s loss [25] (but see [21]). The  
19    larger language models are therefore said to exhibit *emergent capabilities* on complex tasks. More  
20    recently, there has been prevalent discourse in the AI community that further increases in language  
21    model size lead to *plateauing* of performance [6, 20]. Although, there have been attempts to explain  
22    one or two of these empirical phenomena, a unified mathematical framework that explains all three  
23    of these empirically observed phenomena is lacking.

24    To provide simple and insightful explanations of empirical phenomena, several abstract frameworks  
25    have been proposed [2, 15, 17], all based on a skill-text bipartite graph that operates at a semantic  
26    level and captures key real-world properties [26]. Arora and Goyal [2] explain emergent phenomena  
27    by assuming a compute-optimal size scaling rule (Chinchilla allometry rule) [9]. Liao et al. [15] also  
28    assume compute-optimal (Chinchilla) size scaling to explain emergence. Michaud et al. [17] assume  
29    power-law scaling and that each text piece contains only one skill, which may be very different than  
30    real-world scenarios. These existing frameworks explain neither the Chinchilla rule nor the plateau  
31    phenomenon. These three frameworks abstract the gradient dynamics of language model training  
32    [2]; an alternate mathematical framework considers dynamics to explain the Chinchilla rule and loss  
33    function plateaus but does not consider emergence [5].

34    Here we take an approach that builds on information and coding theory [16] that does so, and also  
35    predicts multiple plateaus. In particular, we draw on mathematical ideas around low-density parity  
36    check (LDPC) codes (which achieve Shannon optimality) [23, 19] and random graph theory [3].

37 Though statistical language modeling and information theory were introduced in the same paper [22],  
 38 modern connections between the two are still fairly limited, cf. [4].

39 Our information-theoretic approach is inspired by skill-text bipartite graph frameworks of [2, 15, 17]  
 40 and is closest to [15]. We make a small modification by separating notions of concepts and skills,  
 41 as in well-established human cognitive architectures [18] that have simple hierarchies [14, 1, 13].  
 42 The key difference in our work is to have much more detailed and expressive analysis using non-  
 43 asymptotic techniques rather than asymptotic ones [7]. Indeed, such finitary analysis is necessary  
 44 to even consider size scaling. Recall that [2, 15] assume Chinchilla scaling, whereas we derive it  
 45 without it being built into our framework. Further, with the help of random network theory, we  
 46 provide a simple explanation for emergent abilities of language models in complex tasks when  
 47 their sizes exceed a certain threshold. We show that plateauing of performance with size-scaling  
 48 is just a consequence of diversity of skills required for a task. Moreover, plateauing indicates the  
 49 possibility of multiple emergences as language models continue to scale further. Our work is a step  
 50 in the direction of grounding empirical phenomena observed due to scaling of language models on  
 51 a rigorous mathematical footing. Since our work provides a mathematical explanation for scaling  
 52 laws and emergent abilities, it also helps in policy making by providing insight into the relationship  
 53 between capabilities and resources such as data and compute [10].

## 54 2 Graph-based framework

55 Our framework is based on the notion of learning as two levels. First, a set of concepts are learnt  
 56 from a set of texts with each text involving one or more skills. Second, learning concepts enables the  
 57 language model to acquire skills, and after encountering a sufficient number of texts with co-occurring  
 58 pairs of skills, it eventually acquires compositional abilities resulting in emergent phenomena in  
 59 various complex tasks. The framework naturally leads to information-theoretic analysis in Section 3.

### 60 2.1 Texts, concepts, and skills

61 A set of tokens constitute a text piece from which a language model can learn a wide variety of  
 62 concepts. This is modeled as a concept-text bipartite graph similar to the skill-text bipartite graph in  
 63 [15]. In a given training session (single epoch training), a language model chooses to learn only a  
 64 subset of concepts from a text piece. The total number of skills a model can learn depends on its size.  
 65 Here we consider a hierarchy of skills: basic skills in the first layer and multiple layers of advanced  
 66 skills. Basic skills are easily acquired from concepts, whereas acquiring advanced skills additionally  
 67 requires certain prerequisite skills. We formalize the above notions in the subsequent sections.

### 68 2.2 Notation

69 Let  $\mathcal{T}$  be a subset of text pieces from a set  $\mathfrak{T}$ , and let  $\mathcal{R}$  be a subset of concepts from a set  $\mathfrak{R}$ . Let  
 70 the model size  $N$  (number of parameters) be proportional to the number of concepts  $R = |\mathcal{R}|$ , i.e.,  
 71  $N = \zeta R$ , for some  $\zeta > 0$ .<sup>1</sup> Similarly, let  $\tau$  be the number of tokens in a text piece  $t \in \mathcal{T}$  with  
 72  $T = |\mathcal{T}|$ , implying that the dataset size  $D = \tau T$ . For a given compute budget  $C$ ,<sup>2</sup> a language model  
 73 of size  $N$  can be trained using a dataset of size  $D$  so the constraint  $6ND \leq C$  is satisfied (see [9]).

74 Correspondingly, for a given compute budget,  $G_1^{(C)} = (\mathcal{T} \cup \mathcal{R}, E_{\mathcal{T}\mathcal{R}})$  denotes a concept-text bipartite  
 75 graph, where an edge  $e_{tr} \in E_{\mathcal{T}\mathcal{R}}$  indicates that the language model can learn concept  $r$  from text  
 76  $t$ . Let the degrees of text pieces (number of skills required to understand a text) be binomially  
 77 distributed with a fixed mean degree  $d_t$ , i.e.,  $P_R = \text{Binomial}(n, p) = \text{Binomial}(R, d_t/R)$ . The  
 78 corresponding generating function is  $P_R(x) = \sum_i P_i x^i$ . Let the degree distribution of concepts  
 79 be  $L_T = \text{Binomial}(T, d_r/T)$ , where  $d_r = d_t T/R$ . Note that  $d_t/R = d_r/T =: p$ . There is an  
 80 alternate point of view: If we assume that there exists an edge between a text piece and a concept  
 81 with probability  $d_t/T$ , then a typical graph will have text and concept degree distributions close to  
 82  $P_R$  and  $L_T$ , respectively. It is generally useful to view degree distribution from an edge-perspective,  
 83 which is  $\lambda_T(x) = L'_T(x)/L'_T(1)$  and  $\rho_R(x) = P'_R(x)/P'_R(1)$  [19].

<sup>1</sup>Here, a *concept* is similar to a *skill quantum* in [17].

<sup>2</sup>Compute budget is measured in number of floating point operations or FLOPs [9].

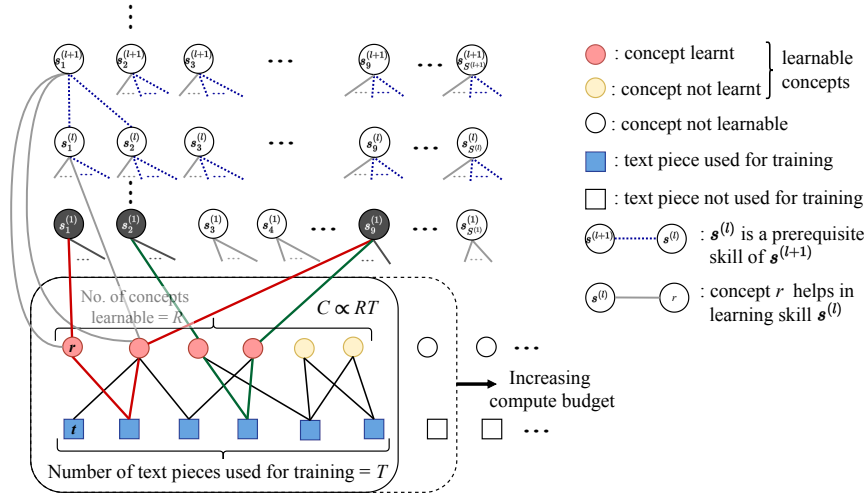


Figure 1: A unified graph-based framework of learning concepts and skills by language models.

84 Let  $G_2 = (\mathfrak{X} \cup \mathcal{S}, E_{\mathfrak{X}\mathcal{S}})$  be a skill-concept graph, where  $\mathcal{S} = \cup_l \mathcal{S}^{(l)}$  denotes a set of hierarchical  
 85 skills, with finite number  $S^{(l)}$  of skills in each level  $l$ . Each concept is connected to a unique skill  
 86 at every level  $l$ , i.e., each concept enables learning of one skill at each level, and each skill  $s^{(l)}$  is  
 87 connected to  $\sigma_l$  prerequisite skills at level  $l - 1$ . Our unified framework is represented by the graph  
 88  $G^{(C)} = G_1^{(C)} \cup G_2$  as shown in Figure 1.

### 89 2.3 Learning concepts from text pieces

90 Following the approach described in [15], we assume that a language model learns concepts from text  
 91 pieces as an iterative peeling process. Let  $\mathcal{R}_+^{(u)}$  denote the set of concepts learnt, and  $\mathcal{R}_-^{(u)}$  denote  
 92 the set of concepts not learnt in peeling iteration  $u$ . Initially, all the concepts are unlearned, i.e.,  
 93  $\mathcal{R}_-^{(0)} = \mathcal{R}$  and  $\mathcal{R}_+^{(0)} = \emptyset$ . Next, a language model learns a concept  $r \in \mathcal{R}_-^{(0)}$  if a text piece  $t \in \mathcal{T}$  is  
 94 uniquely connected to  $r$  yielding  $\mathcal{R}_+^{(1)} = \{r\}$  and  $\mathcal{R}_-^{(1)} = \mathcal{R}_-^{(0)} \setminus \{r\}$ . Before the next iteration, the  
 95 edge  $e_{tr}$  and concept node  $r$  from the graph are removed. The next iteration starts by finding another  
 96 text piece uniquely connected to a concept in  $\mathcal{R}_-^{(1)}$ , and the process continues until there is either no  
 97 more text piece/s connected to a unique concept in  $\mathcal{R}_-$  or all the concepts are learnt, i.e.,  $\mathcal{R}_+ = \mathcal{R}$ .

### 98 2.4 Acquisition of skills and composition of skills

99 A skill  $s^{(l+1)}$  at level  $l+1$  is considered acquired when two conditions hold: 1) all the  $\sigma_{l+1}$  prerequisite  
 100 skills at the lower level  $l$  are learnt, and 2) at least one concept associated with  $s^{(l+1)}$  is learnt. A  
 101 pair of concepts  $(r_1, r_2)$  is considered connected (denoted by  $r_1 - r_2$ ) if there is a path  $r_1 - t - r_2$   
 102 through at least one text  $t \in \mathcal{T}$ . Then, for a fixed level  $l$ , a skill-graph  $G_2^{(l)} = (\mathcal{S}^{(l)}, E_{\mathcal{S}^{(l)} \times \mathcal{S}^{(l)}})$  is  
 103 constructed as follows: A pair of skills  $s_1$  and  $s_2$  in  $\mathcal{S}^{(l)}$  has a direct link (i.e.,  $e_{s_1 s_2} \in E_{\mathcal{S}^{(l)} \times \mathcal{S}^{(l)}}$ )  
 104 if there are at least  $\eta_l$  distinct paths  $s_1^{(l)} - r_1 - r_2 - s_2^{(l)}$  (with at least  $\eta_l$  distinct pairs of concepts  
 105  $(r_1, r_2)$ ), and all the  $2\sigma_l$  prerequisite skills required for both skills are acquired. The intuition behind  
 106 this construction is that a pair of skills is connected (and therefore can be composed) if they co-occur  
 107 sufficiently many times through distinct pairs of concepts in the training data, and all prerequisite  
 108 skills of both skills are already acquired. Further, since more advanced skills are generally hard to  
 109 learn, skills at higher levels (larger values of  $l$ ) need larger values of  $\eta_l$ .

### 110 2.5 Defining emergence

111 As the model size increases there is a sharp increase in performance (e.g. accuracy) of the language  
 112 model on certain complex tasks which the model was not trained on known as emergent phenomena  
 113 in language models [25]. In this context, there are several definitions of skill emergence in the  
 114 literature [2, 15, 21, 17]. In our framework, advanced skills (larger  $l$ ) are acquired from concepts  
 115 and more basic skills, rather than directly from text pieces. To describe the composition of skills not

116 seen in training, we begin by asserting transitivity of skill composition for a fixed skill level  $l$ : if the  
 117 training data contains enough text pieces with composition of both pairs  $(s_1^{(l)}, s_2^{(l)})$  and  $(s_2^{(l)}, s_3^{(l)})$ ,  
 118 then a language model is capable of composing skill  $s_1^{(l)}$  and  $s_3^{(l)}$ . Consequently, a language model  
 119 successfully performs a sub-task requiring a composition of a set of skills  $\mathcal{S}_\theta^{(l)} \subseteq \mathcal{S}^{(l)}$  if there is a  
 120 path between every pair of skills belonging to  $\mathcal{S}_\theta^{(l)}$  in graph  $G_2^{(l)}$ . For small compute budgets, dataset  
 121 size corresponding to compute-optimal performance is small, in which case the training data contains  
 122 composition of only a small number of skill pairs. As compute budget increases, the size of the  
 123 training data increases, and therefore the number of composed skill pairs seen by the language model  
 124 during training increases. Beyond a certain compute-budget threshold and due to skill composition  
 125 transitivity, the ability of the language model to compose most skill pairs emerges, appearing as a  
 126 phase transition around this compute-budget threshold, which we call as skill emergence. As we will  
 127 see in Section 3.3, this phase transition is related to the appearance of a giant connected component  
 128 (GCC) in random graphs with increasing edge probability. Our definition of emergence exhibits phase  
 129 transition as empirically observed in language models, and our finitary analysis helps in conforming  
 130 to the definition of emergence in [25].

### 131 3 Explaining all three phenomena

132 Using the framework in Section 2, we aim to explain the compute-optimal (Chinchilla) scaling rule  
 133 by applying non-asymptotic information-theoretic tools to the bipartite graph  $G_1^{(C)}$ , and explain  
 134 emergence and plateauing phenomena based on the density of connections in the skill-graphs  $\{G_2^{(l)}\}_l$ .

#### 135 3.1 Compute-optimal scaling rule

136 Let  $\mathcal{R}_+ \subseteq \mathcal{R}$  denote the set of concepts learnt after the peeling process terminates. The goal of the  
 137 language model is to maximize the number of concepts learnt under the compute budget constraint  
 138  $C$ , which yields the following constrained optimization problem.

$$\begin{aligned} & \underset{R, T}{\text{maximize}} \mathbb{E}_{G_1^{(C)} \sim (\lambda_T, \rho_R)} [R_+] & (1) \\ & \text{s.t. } RT \leq C', \end{aligned}$$

139 where the number of model parameters  $N = \varsigma R$ , number of tokens in a text piece is  $\tau$ ,  $C' = \frac{C}{6\varsigma\tau}$ ,  
 140 and  $(R^*, T^*)$  is the maximizer of the objective function in (1). For a bipartite graph sampled  
 141 from a degree distribution pair  $(\lambda_T, \rho_R)$ , computing the exact number of learned concepts is  
 142 computationally expensive. Fortunately, the observation that the peeling process is equivalent  
 143 to iterative decoding of LDPC codes when the codeword symbols are corrupted by erasure, al-  
 144 lows us to sidestep this difficulty. Before providing an expression for the objective function,  
 145 some notations are as follows: let  $f(x, \epsilon) = \epsilon\lambda_T(1 - \tilde{\rho}_R(1 - x))$ , then the decoding threshold  
 146  $\epsilon^* = \inf\{\epsilon \in [0, 1] : x = f(x, \epsilon) \text{ has a solution in } x \in (0, 1]\}$ ,  $x^*$  be a critical point satisfying  
 147  $x^* = f(x^*, \epsilon^*)$ ,  $\nu^* = \epsilon^* L_T(1 - \tilde{\rho}_R(1 - x^*))$ . The objective function in (1) is given by (see  
 148 Appendix C.2 for more details):

$$\mathbb{E}_{G_1^{(C)} \sim (\lambda_T, \rho_R)} [R_+] = R \left( 1 - \frac{P_{b, \lambda_T, \tilde{\rho}_R}}{\epsilon} \right) \approx R \left( 1 - \frac{\nu^*}{\epsilon} Q \left( \sqrt{\frac{R}{\epsilon}} \frac{(\epsilon^* - \epsilon)}{\alpha} \right) \right), \quad (2)$$

149 where  $\alpha$  depends on  $(\lambda_T, \tilde{\rho}_R)$ , and  $Q(\cdot)$  is the complementary Gaussian cumulative distribution  
 150 function.

151 Compute optimal size scaling of model size and dataset size with increasing compute budget obtained  
 152 by numerically solving (1) is shown in Figure 2(a) (also see Appendix A for more insights). The  
 153 curves being parallel in logarithmic scale indicates that  $N$  and  $D$  must scale equally with  $C$ . In this  
 154 figure, we set  $\varsigma = 2 \times 10^5$ ,  $\tau = 8 \times 10^5$ , and  $d_t = 6$ . Our finitary analysis also allows us to prove  
 155 the optimality of the Chinchilla rule (see Appendix B).

#### 156 3.2 Scaling of excess entropy

157 Under finitary analysis, for every compute budget  $C$ , there is an associated error rate  $P_{b, \lambda_T, \tilde{\rho}_R}/\epsilon$   
 158 which indicates a fraction of concepts not learnt even after the peeling process is complete. Similar

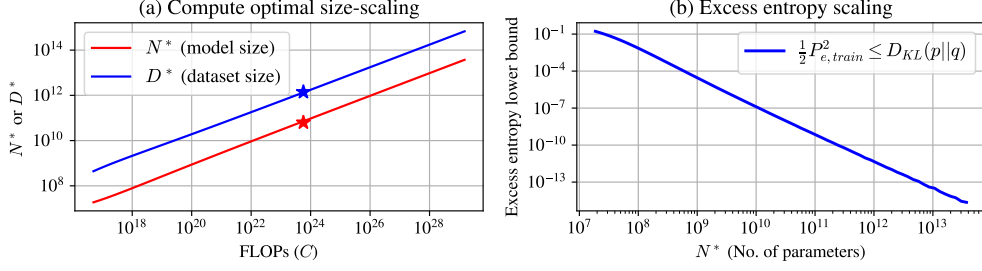


Figure 2: (a) Model and dataset size pair  $(N^*, D^*)$  as a function of compute budget  $C$ . The markers correspond to the Chinchilla model [9] with a compute budget of  $5.76 \times 10^{23}$  FLOPs; (b) Scaling of the lower bound of excess entropy with model size  $N^*$ .

159 to [2], we consider the cloze questions associated with text pieces connected to unlearned concepts  
 160 are incorrectly answered. Therefore, the training error is equivalent to the probability that a check  
 161 node (text piece) is connected to the stopping set (unlearned concepts) at least twice. Refer to [19]  
 162 on stopping sets. The training error corresponding to  $(N, D)$  given a compute budget  $C$  is (see  
 163 Appendix D for the calculation):

$$P_{e,train} = 1 - \left(1 - \frac{d_t P_b}{R}\right)^{R-1} - d_t P_b \left(1 - \frac{d_t P_b}{R}\right)^{R-1} \approx 4d_t^2 \epsilon^{-2} P_{b,\lambda_T,\tilde{\rho}_R}^2. \quad (3)$$

164 Using Pinsker's inequality  $D_{KL}(P||Q) \geq \frac{1}{2} \|P - Q\|_1^2$ , and the equivalence between total variation  
 165 distance and error rate on cloze questions [2], we obtain the following lower bound on excess entropy  
 166 (also shown in Figure 2(b)):

$$\text{Excess entropy} \geq \frac{1}{2} P_{e,train}^2 \approx 2d_t^4 \epsilon^{-4} P_{b,\lambda_T,\tilde{\rho}_R}^4. \quad (4)$$

### 167 3.3 Emergence and plateauing

168 We aim to provide a simple explanation to these empirical phenomena using random graph theory.  
 169 Let  $p_l$  denote the probability there is a direct link between any two pairs of skills at level  $l$ . For a  
 170 fixed  $(R, T)$ ,  $p_l$  evaluates as (see Appendix E for the derivation):

$$p_l \geq \begin{cases} (1 - g(R, p_{rr}, \eta_l)) \gamma_{l-1}^{2\sigma_l} & \text{if } \eta_l \leq \binom{R}{2} p_{rr} \\ \frac{1}{\sqrt{8\eta_l(1-\eta_l/\binom{R}{2})}} g(R, p_{rr}, \eta_l) \gamma_{l-1}^{2\sigma_l} & \text{otherwise,} \end{cases} \quad (5)$$

171 where  $g(R, p_{rr}, \eta_l) = \exp\left(-\binom{R}{2} D_{KL}\left(\frac{\eta_l}{\binom{R}{2}} || p_{rr}\right)\right)$ ,  $p_{rr}$  is the probability that a pair of concepts  
 172 occur in at least one text piece, and  $\gamma_{l-1}$  is the probability that a skill belongs to GCC of  $G_2^{(l)}$  (which  
 173 we show next). Note that the skill graph  $G_2^{(l)}$  is equivalent to an Erdős-Rényi (ER) random graph  
 174 with  $S^{(l)}$  nodes and edge probability  $p_l$ . A pair of skills in level  $l$  can be composed if there is a path  
 175 between them in  $G_2^{(l)}$ , and both skills being in GCC of  $G_2^{(l)}$  is a sufficient condition. Suppose  $\gamma_l$  is  
 176 ratio of the size of GCC in  $G_2^{(l)}$  to  $S^{(l)}$ , and is equivalent to the probability that a skill at level  $l$  is in  
 177 GCC. For an ER graph with edge probability  $p_l$ , solution to  $\gamma_l = 1 - \exp(-p_l S^{(l)} \gamma_l)$  yields  $\gamma_l$  [3]:

$$\gamma_l = 1 + \frac{1}{p_l S^{(l)}} W_0\left(-p_l S^{(l)} \exp\left(-p_l S^{(l)}\right)\right), \quad (6)$$

178 where  $W_0(\cdot)$  is the upper branch of the Lambert  $W$  function. The ratio  $\gamma_l$  has a phase transition at  
 179  $p_l = 1/S^{(l)}$ . To see this, note that  $W_0(xe^x) = x$  for  $x < -1$ . Therefore, whenever  $p_l < 1/S^{(l)}$ ,  $\gamma_l$   
 180 is identically zero. As  $p_l$  increases beyond  $1/S^{(l)}$ ,  $|W_0(\cdot)|$  starts decreasing and  $\gamma_l$  increases.

181 For a particular skill level  $l$ ,  $\gamma_l$  and  $p_l$  can be computed recursively using (6) and (5), with the  
 182 following initial conditions:  $\gamma_0 = 1$  and  $\sigma_l = 0$  (no prerequisite skill is required to learn basic skills,

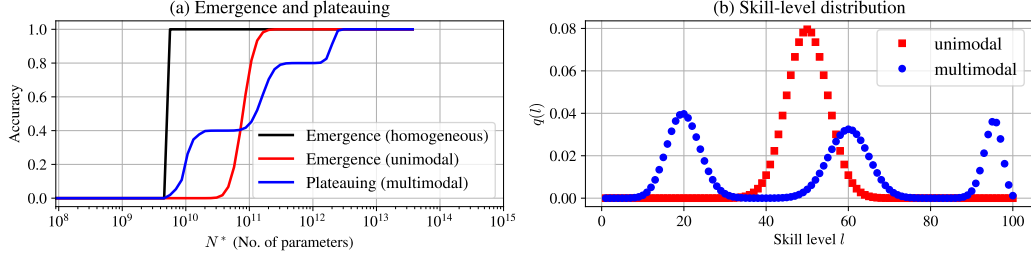


Figure 3: (a) Emergence and performance plateauing for different types of tasks; (b) Skill-level distribution  $q(l)$  for unimodal and multimodal heterogeneous tasks.

183 i.e., skills at  $l = 1$ ). Consider a complex task consisting of subtasks requiring  $m$  skills at level  $l$  with  
 184 probability  $q(l, m)$ . The model performs the subtask successfully only if there is a path between  
 185 every pair of those skills in  $G_2^{(l)}$ . The accuracy of the task is:

$$\text{Accuracy} \geq \sum_{l,m} q(l, m) \gamma_l^m. \quad (7)$$

186 Next, we demonstrate numerically fast emergence (similar to phase transition), slow emergence, and  
 187 plateauing (multiple emergences) are consequences of tasks with different choices of  $q(m, l)$ . For  
 188 illustration, let  $q(m, l) = q(m)q(l)$ , and  $q(m) = 1/6$  for all  $m \in \{2, \dots, 7\}$ , number of skill levels  
 189  $L = 100$ ,  $S^{(l)} = 10^3$ ,  $\eta_l = \exp(7l/L)$ ,  $\sigma_l = \log_2(l)$  for all  $l \in \{1, \dots, L\}$ . Consider a homogeneous  
 190 task requiring skills at only one level, say  $l = 10$ , then the accuracy (according to (7)) exhibits a  
 191 step phase transition with increasing model size (black curve in Figure 3(a)). However, empirically  
 192 observed accuracy curves exhibit smoother phase transitions [25]. To demonstrate this, consider a  
 193 heterogeneous task with binomial distribution over the skill levels, i.e.,  $q(l) = \binom{L}{l} (\frac{1}{2})^L$  (red curve  
 194 in Figure 3(b)). The corresponding accuracy is shown by the red curve in Figure 3(a). In general, a  
 195 smooth single phase transition can be obtained by a unimodal distribution over skill levels with a  
 196 sufficiently large variance. Finally, consider a heterogeneous task with diverse tasks characterized  
 197 by a mixture of binomial distributions over the skill levels, i.e.,  $q(l) = \sum_i w_i \text{Binomial}(L, \pi_i)$ , with  
 198  $(w_i)_i \in (2/5, 2/5, 1/5)$  and  $(\pi_i)_i = (0.2, 0.6, 0.95)$  (blue curve in Figure 3(b)). The blue curve  
 199 in Figure 3(a) shows the corresponding accuracy. In general, a multimodal distribution over skill  
 200 levels results in emergence at multiple scales and plateaus between them. Our framework yields an  
 201 interesting trend associated with the plateauing of performance: plateauing indicates the possibility  
 202 of one (or more) upcoming emergent phenomenon (phenomena), which one would encounter with  
 203 further scaling.

## 204 4 Conclusion

205 We presented a simple unified framework to explain all three empirical phenomena observed with size  
 206 scaling of language models. Existing frameworks assume compute-optimal scaling rule to explain  
 207 emergent phenomena. We use non-asymptotic information theory to explain both compute-optimal  
 208 size scaling and emergent abilities of language models. Moreover, we explain more recent empirical  
 209 phenomenon of plateauing of performance using random network theory, and also predict that  
 210 plateauing implies the possibility of multiple emergent phenomena with further size scaling.

211 There are some open questions and considerations worth exploring. Since, we do not consider training  
 212 time in our framework, we do not explain other empirical phenomena such as double descent or  
 213 grokking [11]. Perhaps future work can either extend our framework or propose a different framework  
 214 to explain them. Even though the sequential learning of concepts through peeling yields a certain  
 215 ordering to concepts, there is no inherent ordering and we do not consider concept hierarchies [27, 28].  
 216 One can explore the advantages of doing so. Evidently, the degree distribution of texts is related to the  
 217 model's architecture. Therefore, optimizing the degree distribution enables a language model to learn  
 218 more concepts from text pieces. Further, the quality of the training data is related to text-to-concept  
 219 edge deletions in sequential concept learning, which can be incorporated into our framework. This  
 220 is a line of future work that has natural analogues in optimization of communication systems and  
 221 fault-tolerant computation.

## 222 **Acknowledgment**

223 We appreciate discussion with and valuable suggestions from Razan Baltaji, Akhil Bhimaraju, and  
224 Moulik Choraria.

225 This work was supported in part by National Science Foundation grant PHY-2112890 and by DARPA  
226 grant “Modeling and Measuring Scientific Creativity”.

## 227 **References**

- 228 [1] John R. Anderson. *Rules of the Mind*. Lawrence Erlbaum Associates, Inc., 1993.
- 229 [2] Sanjeev Arora and Anirudh Goyal. A theory for emergence of complex skills in language  
230 models. arXiv:2307.15936, July 2023.
- 231 [3] Albert-László Barabási. *Network Science*. Cambridge University Press, 2016.
- 232 [4] Sourya Basu, Moulik Choraria, and Lav R. Varshney. Transformers are universal predictors. In  
233 *Neural Compression Workshop (ICML 2023)*, July 2023.
- 234 [5] Blake Bordelon, Alexander Atanasov, and Cengiz Pehlevan. A dynamical model of neural  
235 scaling laws. In *Proceedings of the 41st International Conference on Machine Learning*, pages  
236 4345–4382, July 2024.
- 237 [6] Steven Byrnes. AI doom from an LLM-plateau-ist perspective, 2023.
- 238 [7] Changyan Di, David Proietti, I. Emre Telatar, Thomas J. Richardson, and Rüdiger L. Urbanke.  
239 Finite-length analysis of low-density parity-check codes on the binary erasure channel. *IEEE*  
240 *Transactions on Information Theory*, 48(6):1570–1579, 2002.
- 241 [8] J. B. S. Haldane. On being the right size. *Harper’s Magazine*, pages 425–427, March 1926.
- 242 [9] Jordan Hoffmann, Sebastian Borgeaud, Arthur Mensch, Elena Buchatskaya, Trevor Cai, Eliza  
243 Rutherford, Diego de Las Casas, Lisa Anne Hendricks, Johannes Welbl, Aidan Clark, Tom  
244 Hennigan, Eric Noland, Katie Millican, George van den Driessche, Bogdan Damoc, Aurelia  
245 Guy, Simon Osindero, Karen Simonyan, Erich Elsen, Jack W. Rae, Oriol Vinyals, and Laurent  
246 Sifre. Training compute-optimal large language models. arXiv:2203.15556, March 2022.
- 247 [10] Sara Hooker. On the limitations of compute thresholds as a governance strategy.  
248 arXiv:2407.05694 [cs.AI], July 2024.
- 249 [11] Yufei Huang, Shengding Hu, Xu Han, Zhiyuan Liu, and Maosong Sun. Unified view of  
250 grokking, double descent and emergent abilities: A comprehensive study on algorithm task. In  
251 *Proceedings of the Conference on Language Modeling*, October 2024.
- 252 [12] Jared Kaplan, Sam McCandlish, Tom Henighan, Tom B Brown, Benjamin Chess, Rewon Child,  
253 Scott Gray, Alec Radford, Jeffrey Wu, and Dario Amodei. Scaling laws for neural language  
254 models. arXiv:2001.08361, January 2020.
- 255 [13] Davis E. Kieras and Davis E. Meyer. An overview of the EPIC architecture for cognition and  
256 performance with application to human-computer interaction. *Human-Computer Interaction*,  
257 12(4):391–438, 1997.
- 258 [14] John E. Laird, Allen Newell, and Paul S. Rosenbloom. SOAR: An architecture for general  
259 intelligence. *Artificial Intelligence*, 33(1):1–64, September 1987.
- 260 [15] Kuo-Yu Liao, Cheng-Shang Chang, and Y.-W. Peter Hong. A mathematical theory for learning  
261 semantic languages by abstract learners. arXiv:2404.07009, April 2024.
- 262 [16] Robert J. McEliece. *The Theory of Information and Coding*. Cambridge University Press, 2nd  
263 edition, 2002.

- 264 [17] Eric Michaud, Ziming Liu, Uzay Girit, and Max Tegmark. The quantization model of neural  
 265 scaling. In A. Oh, T. Naumann, A. Globerson, K. Saenko, M. Hardt, and S. Levine, editors,  
 266 *Advances in Neural Information Processing Systems*, volume 36, pages 28699–28722. Curran  
 267 Associates, Inc., 2023.
- 268 [18] Allen Newell. *Unified Theories of Cognition*. Harvard University Press, 1990.
- 269 [19] Tom Richardson and Rüdiger Urbanke. *Modern Coding Theory*. Cambridge University Press,  
 270 2008.
- 271 [20] Gordon Ritter and Wendy Lu. The first wave of AI innovation is over. here’s what comes next.  
 272 *Fast Company*, July 2024.
- 273 [21] Rylan Schaeffer, Brando Miranda, and Sanmi Koyejo. Are emergent abilities of large language  
 274 models a mirage? In A. Oh, T. Naumann, A. Globerson, K. Saenko, M. Hardt, and S. Levine,  
 275 editors, *Advances in Neural Information Processing Systems*, volume 36, pages 55565–55581.  
 276 Curran Associates, Inc., 2023.
- 277 [22] Claude E. Shannon. A mathematical theory of communication. *Bell System Technical Journal*,  
 278 27(3/4):379–423/623–656, July/October 1948.
- 279 [23] Nicolas Sourlas. Spin-glass models as error-correcting codes. *Nature*, 339:693–695, June 1989.
- 280 [24] D’Arcy Wentworth Thompson. *On Growth and Form*. Cambridge University Press, 1917.
- 281 [25] Jason Wei, Yi Tay, Rishi Bommasani, Colin Raffel, Barret Zoph, Sebastian Borgeaud, Dani  
 282 Yogatama, Maarten Bosma, Denny Zhou, Donald Metzler, Ed H. Chi, Tatsunori Hashimoto,  
 283 Oriol Vinyals, Percy Liang, Jeff Dean, and William Fedus. Emergent abilities of large language  
 284 models. arXiv:2206.07682, June 2022.
- 285 [26] Dingli Yu, Simran Kaur, Arushi Gupta, Jonah Brown-Cohen, Anirudh Goyal, and Sanjeev Arora.  
 286 Skill-Mix: a flexible and expandable family of evaluations for AI models. arXiv:2310.17567,  
 287 October 2023.
- 288 [27] Haizi Yu, James A. Evans, and Lav R. Varshney. Information lattice learning. *Journal of*  
 289 *Artificial Intelligence Research*, 77:971–1019, 2023.
- 290 [28] Haizi Yu, Igor Mineyev, and Lav R. Varshney. A group-theoretic approach to computational  
 291 abstraction: Symmetry-driven hierarchical clustering. *Journal of Machine Learning Research*,  
 292 24(47):1–61, 2023.

## 293 5 Appendix

### 294 A IsoFLOP curves

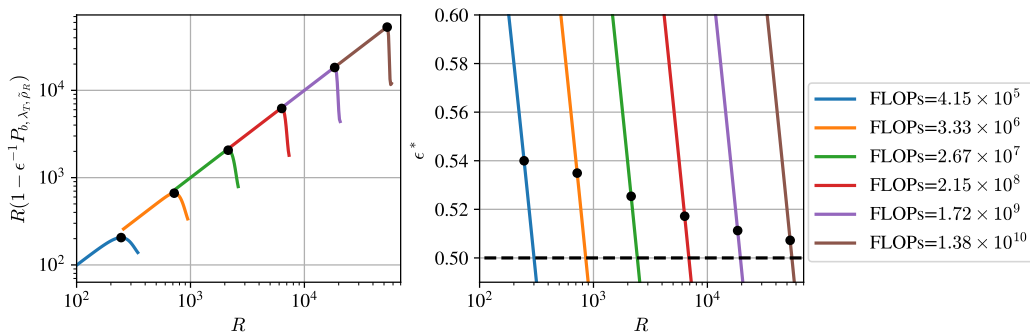


Figure 4: **IsoFLOP curves**: (left) Number of concepts learnt as a function of  $R$  for different compute budget; (right) Block erasure threshold as a function of the number of concepts  $R$  for different compute budget. In both subfigures, solid black markers indicate the points corresponding to  $R^*$ .



295 In Figure 4, the objective function in (1) is plotted against the number of concepts  $R$  for multiple  
 296 compute budgets. In the left subfigure, each curve corresponds to a fixed compute budget. Note  
 297 that smaller values of  $R$  correspond to smaller language model sizes, in which case the dataset size  
 298 (number of texts  $T$ ) is more than necessary for the model to learn all the skills. Contrarily, for large  
 299 model sizes, the smaller dataset size is insufficient to learn the concepts well. There is an optimum  
 300 model size and dataset size pair (equivalently  $R$  and  $T$ ) such that the number of concepts learnt is  
 301 maximized, as indicated by a solid black marker for each compute budget  $C$ . This figure is analogous  
 302 to isoFLOP curves in [9, Figure 2], where training loss is plotted against model size for different  
 303 compute budgets.

## 304 B Optimality of Chinchilla scaling rule

305 **Proposition 1. Compute-optimal scaling rule:** For compute-optimal performance of a language  
 306 model, the dataset size ( $D$ ) and model size ( $N$ ) must scale equally with the increasing compute  
 307 budget  $C$  (or FLOPs).

308 *Proof.* The approach is to prove that neither  $T/R = o(1)$  nor  $R/T = o(1)$  maximizes the objective  
 309 function in (1). This implies that  $R/T$  must be a constant, i.e.,  $R$  and  $T$  must scale equally with  
 310 compute budget  $C$ .

311 Denote  $\epsilon^*$  be the decoding threshold corresponding to the degree distribution pair  $(\lambda_T, \tilde{\rho}_R)$ . From  
 312 the matching condition [19], we have

$$\epsilon^* \leq \frac{\int \tilde{\rho}_R}{\int \lambda_T} =: \epsilon_{ub}^*$$

313 (a) If  $\frac{T}{R} = o(1)$  (i.e.,  $\frac{T}{R}$  decays as  $C \rightarrow \infty$ ), then

$$\epsilon_{ub}^* - \epsilon \leq \epsilon \left( \left( 1 - e^{-d/\epsilon} + \frac{d^2}{\epsilon R} \right) \left( \frac{1}{d} + \frac{T}{R} \right) - 1 \right) \xrightarrow{C \rightarrow \infty} \epsilon \left( \frac{(1 - e^{-d/\epsilon})}{d} - 1 \right) < 0,$$

314 which implies that  $P_{b, \lambda_T, \tilde{\rho}_R} \rightarrow 1$ . Therefore, number of skills learnt vanishes for large  $C$ .

315 (b) Consider  $\frac{R}{T} = o(1)$ . From the fixed point characterization of decoding threshold of LDPC  
 316 codes, we have

$$\begin{aligned} f(x, \epsilon^*) &= \epsilon^* \lambda_T (1 - \tilde{\rho}_R (1 - x)), \\ &= \epsilon^* (1 - (1 - xp)^{\frac{R}{\epsilon} - 1} p)^{T-1}, \end{aligned} \quad (8)$$

317 where  $p = d_t/R$ . Since  $R/T = o(1)$ , the number of text pieces  $T$  grows strictly faster  
 318 than  $R$  with respect to compute budget  $C$ , implying that the second term in (8), i.e.,  
 319  $(1 - (1 - xp)^{\frac{R}{\epsilon} - 1} p)^{T-1} \rightarrow 0$  for large  $C$ . Therefore, for a non-trivial solution, i.e.,  
 320  $x = f(x, \epsilon^*) \in (0, 1]$ , the decoding threshold  $\epsilon^*$  must be very large. As a result, the  
 321 post-decoding bit erasure rate  $P_{b, \lambda_T, \tilde{\rho}_R}$  vanishes for large  $C$ .

322 Suppose,  $(R_C^*, T_C^*)$  such that  $R_C^*/T_C^* = o(1)$  minimizes (1). Now, consider  $\hat{R}_C = R_C^*(1 + \delta)$   
 323 and  $\hat{T}_C = T_C^*/(1 + \delta)$ . Note that  $\hat{R}_C/\hat{T}_C = (1 + \delta)^2 R_C^*/T_C^* = o(1)$ . Therefore, for any  
 324  $\delta' \in (0, \delta)$ , there exists  $C_0$  such that for all  $C \geq C_0$  the bit erasure rate  $\epsilon^{-1} P_{b, \lambda_{\hat{T}_C}, \tilde{\rho}_{\hat{R}_C}} \leq$   
 325  $\delta'/(1 + \delta')$ . Now consider the ratio of number of concepts learnt:

$$\frac{\hat{R}_C (1 - \epsilon^{-1} P_{b, \lambda_{\hat{T}_C}, \tilde{\rho}_{\hat{R}_C}})}{R_C^* (1 - \epsilon^{-1} P_{b, \lambda_{T_C^*}, \tilde{\rho}_{R_C^*}})} \geq \frac{R_C^* (1 + \delta) \left( 1 - \frac{\delta'}{1 + \delta'} \right)}{R_C^*} = \frac{1 + \delta}{1 - \delta'} > 1, \quad (9)$$

326 where the first inequality is by substitution and using the fact that  $\epsilon^{-1} P_{b, \lambda_{\hat{T}_C}, \tilde{\rho}_{\hat{R}_C}}$  is non-  
 327 negative, and the second inequality is because  $\delta' < \delta$ . Therefore,  $(R_C^*, T_C^*)$  is not a  
 328 maximizer, which is a contradiction. Therefore,  $R/T$  cannot be  $o(1)$ .

329 Therefore,  $R/T$  must asymptotically be a constant. In other words, the model size  $N$  and dataset size  
 330  $D$  must scale equally with compute budget  $C$ .

331 □

332 **C Solving (1): Maximizing concept learning under compute budget constraint**

333 **C.1 A brief summary of belief propagation decoding of LDPC codes under erasure**

334 Low-density parity check (LDPC) codes are a family of error-correction codes, whose noisy code-  
 335 words can be decoded in a computationally efficient manner using belief propagation. Before getting  
 336 into deriving the probability that a concept is learnt from text pieces, we provide a very short summary  
 337 of belief propagation decoding of LDPC codes when codeword symbols are corrupted by erasure. An  
 338 LDPC code can be graphically represented by a Tanner graph, which is a bipartite graph with a set of  
 339 variable nodes (codeword symbols) and check nodes (parity checks). Each codeword satisfies all the  
 340 parity checks. Given a degree distribution pair (for variable and check nodes), there is a channel noise  
 341 threshold  $\epsilon^*$  above which the decoder fails to decode the transmitted codeword. Consider a noisy  
 342 version of a transmitted codeword with  $\epsilon < \epsilon^*$  fraction of the symbols are erased. Belief propagation  
 343 decoding starts by finding a check node where all except one symbol are recieved correctly (not  
 344 erased). Then the erased symbol is determined as the one satisfying the parity. The next iteration  
 345 starts by finding another check node with only one erased codeword symbol. This process continues  
 346 until either all the codeword symbols are decoded or the decoder gets stuck with no parity checks  
 347 containing only one erased symbol. The latter is declared as a decoding failure.

348 **C.2 Computing  $\mathbb{E}_{G_1^{(C)} \sim (\lambda_T, \rho_R)}[R_+]$**

349 The objective function in (1) can be rewritten as:

$$\mathbb{E}_{G_1^{(C)} \sim (\lambda_T, \rho_R)}[R_+] = R(1 - \Pr\{r \notin \mathcal{R}_+ | R, T\}). \quad (10)$$

350 where  $\Pr\{r \notin \mathcal{R}_+ | R, T\}$  is the probability that a concept  $r$  is remains unlearnt after peeling.  
 351 Learning concepts from texts by the peeling process described in Section 2.3 is identical to belief  
 352 propagation decoding of an LDPC code when the channel noise is erasure. To see this, treat  
 353  $R$  concepts as erased codeword symbols (subset of variable nodes), and  $T$  text pieces as parity  
 354 checks. To obtain one-to-one correspondence, we need un-erased symbols (the remaining subset  
 355 of variable nodes). Therefore, we choose (arbitrarily) a channel noise parameter  $\epsilon \in (0, 1)$ , add  
 356  $\frac{1-\epsilon}{\epsilon}R$  nodes (dummy nodes) to the set of variable nodes, and treat them as un-erased symbols. Next,  
 357 add edges between every pair of dummy variable node and a parity check node with probability  
 358  $p = \frac{d_t}{R}$ . Consequently, the degree distribution of the parity check nodes (text pieces) is modified,  
 359 i.e., its degree distribution is binomial with parameters  $R/\epsilon$  (instead of  $R$ ) and  $d_t/R$ , but the degree  
 360 distribution of variable nodes remains unchanged. Let us call the resulting parent graph  $\tilde{G}_1^3$  (see  
 361 Figure 5) with the following text and concept degree distributions,

$$\tilde{P}_R = \text{Binomial}(R/\epsilon, p), \text{ and} \quad (11)$$

$$\tilde{L}_T = L_T = \text{Binomial}(T, p), \quad (12)$$

362 respectively. Here, for a compute budget  $C$ , we set  $T = \frac{C}{6\varsigma\tau R}$ .

---

<sup>3</sup>In this section, we omit superscript  $(C)$  in  $\tilde{G}_1^{(C)}$  for brevity.

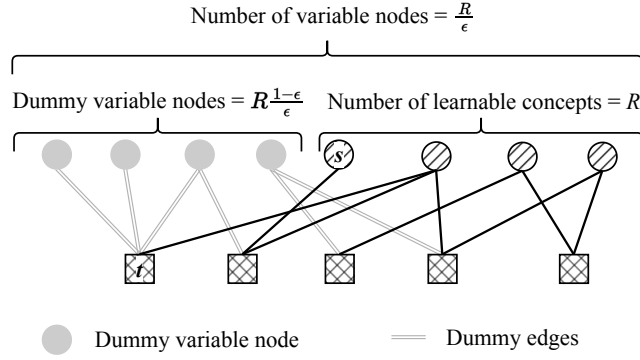


Figure 5: Bipartite graph  $\tilde{G}_1$ .

363 In belief propagation decoding (peeling) of a codeword affected by erasures, the post-decoding bit  
 364 erasure rate depends only on the residual graph consisting only variable nodes corresponding to erased  
 365 symbols, parity checks connecting those variable nodes, and edges between them. Therefore, the  
 366 post-decoding bit erasure rate is invariant to the choice of  $\epsilon$ .<sup>4</sup> Therefore, we can make the following  
 367 equivalence between concept learning and bit erasure rate:

$$\Pr\{r \notin \mathcal{R}_+ | R, T\} = \frac{P_{b, \lambda_T, \tilde{\rho}_R}}{\epsilon}, \quad (13)$$

368 where  $P_{b, \lambda_T, \tilde{\rho}_R}$  is the post-decoding bit erasure rate, and  $\lambda_T(x) = \frac{L'_T(x)}{L'_T(1)}$  and  $\tilde{\rho}_R(x) = \frac{\tilde{P}'_R(x)}{\tilde{P}'_R(1)}$   
 369 are variable and check node degree distributions from edge perspective, respectively. To compute  
 370  $P_{b, \lambda_T, \tilde{\rho}_R}$  we need the following ingredients: degree distributions  $\lambda_T$  and  $\tilde{\rho}_R$ , decoding threshold  $\epsilon^*$ ,  
 371 and scaling factors  $\nu^*$  and  $\alpha$  which depend on degree distributions. Degree distribution of text pieces  
 372 from the node perspective is

$$P_R(x) = \sum_i \binom{R}{i} p^i (1-p)^{R-i} x^i, \quad (14)$$

$$\tilde{P}_R(x) = \sum_i \binom{R/\epsilon}{i} p^i (1-p)^{(R/\epsilon)-i} x^i, \quad (15)$$

373 which gives the following text degree distribution from the edge perspective:

$$\tilde{\rho}_R(x) = \frac{\tilde{P}'_R(x)}{\tilde{P}'_R(1)} = \frac{\sum_i i \binom{R/\epsilon}{i} p^i (1-p)^{(R/\epsilon)-i} x^{i-1}}{\sum_i i \binom{R/\epsilon}{i} p^i (1-p)^{(R/\epsilon)-i}}. \quad (16)$$

374 Noting that  $i \binom{R/\epsilon}{i} = R \binom{R/\epsilon-1}{i-1}$  we obtain the degree distribution of text pieces from edge perspective:

$$\tilde{\rho}_R(x) = \frac{\sum_{j=0}^{(R/\epsilon)-1} \frac{R}{\epsilon} p \binom{R/\epsilon-1}{j} p^{j-1} (1-p)^{(R/\epsilon)-j} x^{j-1}}{\frac{R}{\epsilon} p} \quad (17)$$

$$= (px + (1-p))^{\frac{R}{\epsilon}-1}. \quad (18)$$

375 Similarly, the degree distribution of concepts (remains unchanged for a fixed  $R, T$ ) from the edge  
 376 perspective is

$$\lambda_T(x) = (px + (1-p))^{T-1}. \quad (19)$$

377 Next the belief propagation decoding threshold  $\epsilon^*$  is obtained from its fixed point characterization  
 378 [19, Section 3.12]:

$$\epsilon^* = \inf\{\epsilon \in [0, 1] : x = f(x, \epsilon) \text{ has a solution in } x \in (0, 1]\}, \quad (20)$$

<sup>4</sup>Here we choose  $\epsilon = 0.5$  (instead of close to 0 or 1) for numerical convenience.

379 where  $f(x, \epsilon) = \epsilon \lambda_T(1 - \tilde{\rho}_R(1 - x))$ , and the critical point  $x^*$  satisfies  $x^* = f(x^*, \epsilon^*)$ .

380 From finite-length scaling law of error rates in belief propagation decoding [19, Section 3.23], we  
381 have the following (approximate) closed-form expression for post-decoding bit erasure rate:

$$P_{b, \lambda_T, \tilde{\rho}_R} \approx \nu^* Q \left( \sqrt{\frac{R}{\epsilon}} \frac{(\epsilon^* - \epsilon)}{\alpha} \right), \quad (21)$$

382 where  $\nu^* = \epsilon^* L_T(1 - \tilde{\rho}_R(1 - x^*))$ ,  $Q(\cdot)$  is the complementary standard Gaussian cumulative  
383 distribution function, and the scaling parameter  $\alpha$  is given by [19, Section 3.23]

$$\alpha = \left( \frac{\rho(\bar{x}^*)^2 - \rho((\bar{x}^*)^2) + \rho'(\bar{x}^*)(1 - 2x^*\rho(\bar{x}^*)) - (\bar{x}^*)^2 \rho'((\bar{x}^*)^2)}{L_T'(1) \lambda_T(y^*)^2 \rho'(\bar{x}^*)^2} + \right. \quad (22)$$

$$\left. \frac{(\epsilon^*)^2 \lambda(y^*)^2 - (\epsilon^*)^2 \lambda_T((y^*)^2) - (y^*)^2 (\epsilon^*)^2 \lambda_T'((y^*)^2)}{L_T'(1) \lambda(y^*)^2} \right)^{1/2}, \quad (23)$$

384 where  $x^*$  is the unique critical point,  $\bar{x}^* = 1 - x^*$ , and  $y^* = 1 - \tilde{\rho}_R(1 - x^*)$ .

## 385 D Calculation of $P_{e, \text{train}}$

386 Recall that the training error is equivalent to finding the probability that a text piece is connected to  
387 an unlearned concept, i.e.,

$$P_{e, \text{train}} = \Pr \left( |\{e_{tr} \in G_1^{(C)}\}_{r \in \mathcal{R}_-}| \geq 2 \right), \text{ for any } t \in \mathcal{T}, \quad (24)$$

$$= \sum_{k \geq 2}^R \Pr \left( \text{degree}(t) = k, |\{e_{tr} \in G_1^{(C)}\}_{r \in \mathcal{R}_-}| \leq 1 \right)^c, \quad (25)$$

$$= \sum_{k \geq 2}^R \binom{R}{k} p^k (1-p)^{R-k} \left( 1 - (1-P_b)^k - kR(1-P_b)^{k-1} \right), \quad (26)$$

388 where the edge probability  $p = d_t/R$  and  $P_b = \epsilon^{-1} P_{b, \lambda_T, \tilde{\rho}_R}$ . The last equation simplifies to:

$$P_{e, \text{train}} = 1 - \left( 1 - \frac{d_t P_b}{R} \right)^{R-1} - d_t P_b \left( 1 - \frac{d_t P_b}{R} \right)^{R-1}, \quad (27)$$

389 which is obtained by computing the expectation of each of the three terms within the summation in  
390 (26) and substituting  $p = d_t/R$ . Further using the approximations  $(1-x)^n \approx 1-nx$  and  $R-1 \approx R$   
391 for large  $R$ , the training error is approximately  $P_{e, \text{train}} \approx 4d_t^2 P_b^2$ .

## 392 E Calculation of $p_l$

393 Recall that  $p_l$  is the probability that the composition of a pair of skills in level  $l$  is seen at least  $\eta_l$   
394 times in the training data. For a fixed pair of skills  $(s_1, s_2)$ , the probability there is a path between  
395 the pair of skills through some pair of concepts  $(r_1, r_2)$  is

$$\begin{aligned} \Pr(s_1 - r_1 - r_2 - s_2) &= \Pr(s_1 - r_1, r_1 - r_2, r_2 - s_2), \\ &= \Pr(s_1 - r_1) \Pr(r_1 - r_2) \Pr(r_2 - s_2), \\ &= \frac{1}{S^{(l)}} \left( 1 - \left( 1 - \frac{d_t^2}{R^2} \right)^T \right) \frac{1}{S^{(l)}} =: p_{rr}, \end{aligned}$$

396 where the second inequality is due to independence of  $s_1 - r_1$ ,  $r_1 - r_2$  and  $r_2 - s_2$ . Let  $X$  be a  
397 random variable indicating the number of distinct paths  $s_1 - r_1 - r_2 - s_2$  between  $s_1$  and  $s_2$ . Now,  
398  $\Pr(\text{composition of } (s_1, s_2) \text{ in training data}) =: p_l$  is

$$\begin{aligned} p_l &= \Pr(X \geq \eta_l, \text{ all prerequisite skills of } s_1 \text{ and } s_2 \text{ are acquired}), \\ &\geq \Pr(X \geq \eta_l) \Pr(\text{all prerequisite skills of } s_1 \text{ and } s_2 \text{ are acquired}). \end{aligned}$$

399 Note that the total number of distinct paths between  $s_1$  and  $s_2$  equals the total number of concept  
400 pairs  $(r_1, r_2)$  which is  $\binom{R}{2}$ , each with probability  $p_{rr}$ . Therefore,  $X$  follows a binomial distribution,  
401 i.e., Binomial  $\left(\binom{R}{2}, p_{rr}\right)$ . From Chernoff's bound for binomial distribution, we obtain the following  
402 lower bounds:

$$\Pr(X \geq \eta_l) \geq \begin{cases} \left(1 - \exp\left(-\binom{R}{2} D_{KL}\left(\frac{\eta_l}{\binom{R}{2}} \parallel p_{rr}\right)\right)\right) & \text{if } \eta_l \leq \binom{R}{2} p_{rr} \\ \frac{1}{\sqrt{8\eta_l \left(1 - \frac{\eta_l}{\binom{R}{2}}\right)}} \exp\left(-\binom{R}{2} D_{KL}\left(\frac{\eta_l}{\binom{R}{2}} \parallel p_{rr}\right)\right) & \text{otherwise.} \end{cases} \quad (28)$$

403 The probability of acquiring prerequisite skills of both skills  $s_1$  and  $s_2$  is (assuming  $R \gg \sigma_l$ ),

$$\begin{aligned} \Pr(\text{all prerequisite skills of } s_1 \text{ and } s_2 \text{ are acquired}) &\geq \Pr(\text{all } \sigma_l \text{ prerequisites} \in \text{GCC})^2, \\ &= \gamma_{l-1}^{2\sigma_l}. \end{aligned}$$